Monthly Notices
of the
ROYAL ASTRONOMICAL SOCIETY

MNRAS **482,** 2893–2901 (2019)
Advance Access publication 2018 October 18

doi:10.1093/mnras/sty2803

Observability of molecular species in a nitrogen dominated atmosphere for 55 Cancri e

Y. Miguel★

Leiden Observatory, University of Leiden, Niels Bohrweg 2, 2333CA Leiden, The Netherlands

Accepted 2018 October 5. Received 2018 October 3; in original form 2018 August 22

ABSTRACT

One of the key goals of exoplanet science is the atmospheric characterization of super-Earths. Atmospheric abundances provide insight on the formation and evolution of those planets and help to put our own rocky planets in context. Observations on 55 Cancri e point towards an N-dominated atmosphere. In this paper we explore this possibility, showing which will be the most abundant gases and observable species in emission and transmission spectroscopy of such an atmosphere. We use analytical arguments and observed parameters to estimate the possible thermal profile of the atmosphere and test three different extreme possibilities. The chemistry is calculated using equilibrium calculations and adopting Titan's elemental abundances as a potential N-dominated atmospheric composition. We also test the effect of different N/O ratios in the atmosphere. Emission and transmission spectra are computed and showed with a resolution relevant to future missions suitable to observe super-Earths (e.g. JWST, ARIEL). We find that even though N_2 is the most abundant molecule in the atmosphere followed by H_2 and CO, the transmission spectra show strong features of NH_3 and HCN, and CO and HCN dominate emission spectra. We also show that a decrease in the N/O ratio leads to stronger H_2O, CO and CO_2 and weaker NH_3 and HCN features. A larger N/O is also more consistent with observations. Our exploration of an N-atmosphere for 55 Cancri e serve as a guide to understand such atmospheres and provide a reference for future observations.

Key words: planets and satellites: atmospheres – planets and satellites: composition – planets and satellites:detection.

1 INTRODUCTION

Characterizing exoplanet's atmospheres is the new frontier in exoplanet studies. The knowledge of abundances of molecular species on exoplanet atmospheres may reveal how the planet was formed and evolved (Öberg, Murray-Clay & Bergin 2011; Cridland, Pudritz & Alessi 2016; Espinoza et al. 2017; Madhusudhan et al. 2017). While many hot-Jupiters have been observed, the great observational challenges of detecting atmospheres in small, mini-gas and rocky planets make their atmospheric properties highly unknown.

55 Cancri e (also called Janssen) is a super-Earth of $8.703M_\oplus$ and $2.023R_\oplus$ (Crida et al. 2018) located at 0.0154 au from its host star (Nelson et al. 2014). Radius and mass measurements combined with interior model calculations suggest that the planet might have a high-mean-molecular-weight atmosphere (Demory et al. 2011; Winn et al. 2011; Bourrier et al. 2018). This scenario is also supported by Ly α observations, which show that the planet does not have a light H-dominated atmosphere (Ehrenreich et al. 2012). The high temperatures observed (1300–2800K; Demory et al. 2011) led to the thought that it might have outgassing that enriches a primary solar-composition atmosphere (Mahapatra, Helling & Miguel 2017) or might be essentially a rock with a small heavy Na-dominated outgassed atmosphere (Miguel et al. 2011; Schaefer & Fegley 2009). Nevertheless, the search for Na in its atmosphere with high-resolution spectroscopy was non-conclusive (Ridden-Harper et al. 2016). Other searches for molecular features using transit spectroscopy (Tsiaras et al. 2016) and high-resolution spectroscopy (Esteves et al. 2017) turn out also with non-conclusive results. Better constrains were obtained with recent phase curve observations (Demory et al. 2016), and a subsequent re-analysis of these observations by Angelo & Hu (2017) and 3D calculations by Hammond & Pierrehumbert (2017), which show that the peak of the planet's radiation observed prior to the occultation, and the large day–night temperature contrast might be explained with an N-dominated atmosphere.

Based on these last results, the aim of this paper is to explore the most relevant features in the spectra and potential observability of molecular species in an N-dominated atmosphere for 55 Cancri e. While detailed interior composition and posterior evolution and

★ E-mail: ymiguel@strw.leidenuniv.nl

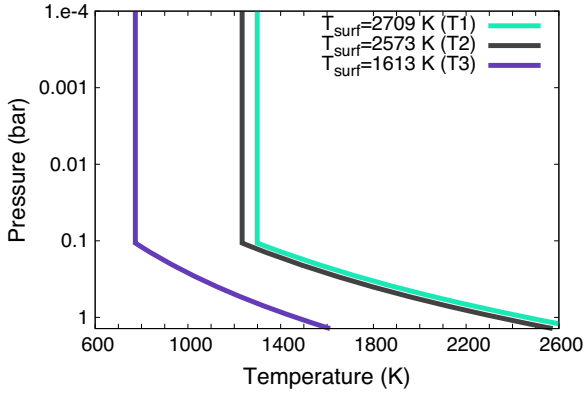

Figure 1. Temperature and pressure profiles for 55 Cancri e derived using an analytic formulae and parameters from Angelo & Hu (2017) (see text). The three profiles represent extreme possibilities derived from observations, using a maximum temperature (T1, green), a mean value (T2, grey) and a minimum temperature (T3, purple).

formation of the atmosphere is largely unknown and out of the scope of this work, we study the spectral features of an N-dominated atmosphere using Titan's elemental abundances composition and explore the effect of different N/O ratios. We calculate the most abundant elements for such atmosphere exploring different thermal profiles and model emission and transmission spectra between 3 and 20 μm to analyse the potential observability with future instrumentation such as the MIRI instrument on JWST and ARIEL.

2 ATMOSPHERIC MODEL

2.1 Thermal profile

The thermal profile of 55 Cancri e is estimated using an analytical approach, where the temperature follows a dry adiabatic profile (Pierrehumbert 2010) from a pressure of 1.4 bar (Angelo & Hu 2017) until 0.1 bar and an isothermal profile for lower pressures, following the approach by Morley et al. (2017) for small rocky exoplanets.

$$T(P) = \begin{cases} \text{Isothermal} & \text{if } P \leq 0.1\text{bar}, \\ T_{\text{surf}} \left(\frac{P}{1.4\text{ bar}}\right)^{\frac{R}{c_P}} & \text{if } 0.1 < P \leq 1.4\text{bar}. \end{cases} \quad (1)$$

For this calculation, we assume that the atmosphere is made of N_2 and for the temperature at the surface, we use the values derived in Angelo & Hu (2017), which calculated a maximum hemisphere-averaged temperature of ≃2709K (hereafter T1), an average dayside temperature of ≃2573K (T2) and a minimum hemisphere-averaged temperature of ≃1613K (T3). Given that we are using an approximated thermal profile, we explore different, extreme possibilities, to explore potential changes in the spectral features due to this approximation. The three atmospheric profiles used in the paper are shown in Fig. 1.

2.2 Atmospheric chemistry

Recent observations of 55 Cancri e suggest the possibility of a high-mean-molecular-weight atmosphere (Ehrenreich et al. 2012; Demory et al. 2016). Furthermore, the analysis performed by Angelo & Hu (2017), suggests that the planet might have an N_2-dominated atmosphere with a small percentage of H_2O and CO_2. To study this scenario, and as a proxy for an N_2-dominated atmosphere,

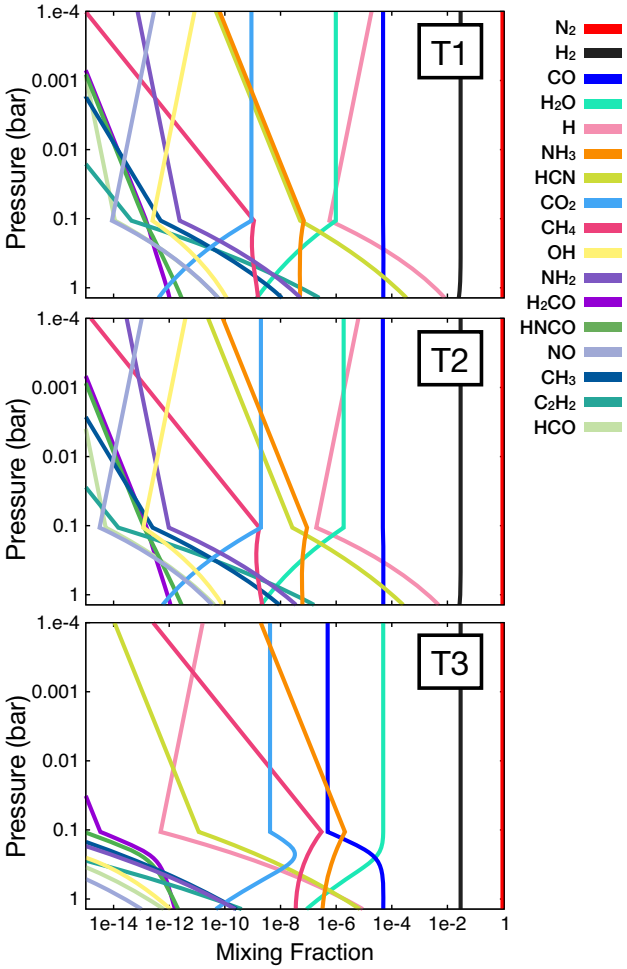

Figure 2. Mixing fraction of each gas as a function of atmospheric pressure. We show results using three different thermal profiles as input: profile T1 (top), T2 (medium) and T3 (bottom panel).The most abundant gases are shown with different colours as indicated, where the species in the label are written in order from high to low abundance for profile T2 at 0.01 bar.

we use the elemental abundances in Titan's atmosphere, where the mole fractions of each element are N=0.96287, H=0.03, C=0.007 and O = 2.5e-5 (Morley et al. 2017). Since the atmospheric composition of 55 Cancri e is highly unknown, in Section 3.1 we also consider two other atmospheric compositions, keeping an N-dominated atmosphere but changing the N/O ratio. We calculate the abundance of the gases in the atmosphere using the equilibrium chemistry code TEA, which computes the final mixing fractions using the Gibbs free-energy minimization method (Blecic, Harrington & Bowman 2016).

Fig. 2 shows mixing fractions of the most abundant gases in the atmosphere. These abundances depend on the thermal profile, therefore we see differences between the three cases. For all profiles N_2 is the most abundant gas in the atmosphere with a mixing fraction of ∼0.956, followed by H_2 (for all pressures). Cases T1 and T2 have a high CO abundance close to 5×10^{-5} (for all pressures), while for T3 CO abundance is two orders of magnitude lower ($\sim 5 \times 10^{-7}$, for P<0.1 bar). T3 profile has a lower temperature that favours the formation of H_2O for pressures lower than 0.1 bar (mixing fraction of $\sim 5 \times 10^{-5}$), while H_2O abundance is lower for T1 and T2 (mixing fraction of $\sim 2 \times 10^{-6}$). Other abundant gases for N-chemistry are NH_3 and HCN, which are also seen in the spectra (see Section 3).

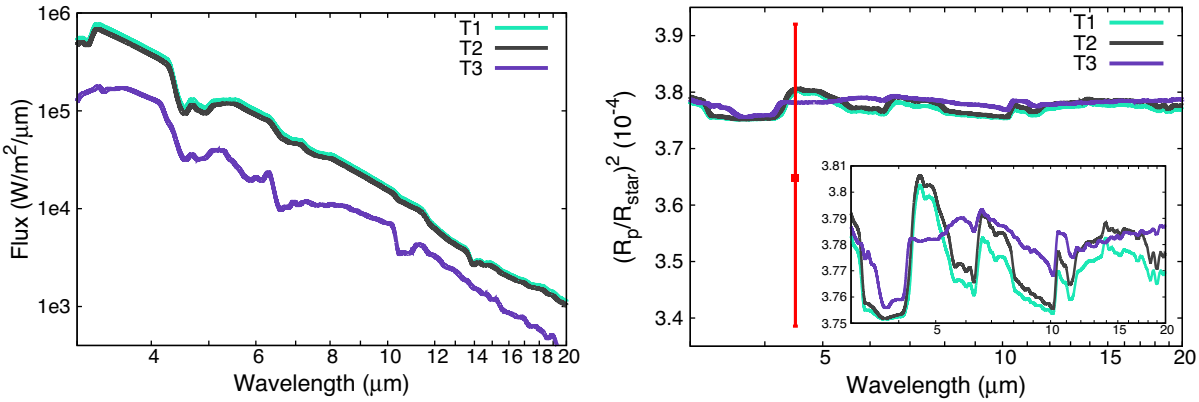

Figure 3. Emission (left) and transmission (right panel) synthetic spectra of 55 Cancri e between 3 and 20 μm for the three thermal profiles and same colour scheme shown in Fig. 1. The red point in the right panel shows the average transit depth of 55 Cnc e observed with *Spitzer* (Demory et al. 2016).

2.3 Synthetic spectra

The synthetic spectra of 55 Cancri e are calculated using the Smithsonian Astrophysical Observatory 1998 (SAO98) line-by-line radiative transfer code, originally built for Earth like planets (Traub & Stier 1976; Traub & Jucks 2002; Kaltenegger, Traub & Jucks 2007) and subsequently tested and used in multiple papers for rocky exoplanets (Kaltenegger & Traub 2009; Rugheimer et al. 2013; Rugheimer & Kaltenegger 2018) and recently adapted for hot-Jupiter modelling (Wang, Miguel & Lunine 2017). We calculate emission and transmission spectra at high resolution (0.1 cm^{-1} wavenumber steps) and smear them out to a resolving power of 100 to simulate the resolution that we will obtain with the MIRI instrument on JWST, (Greene et al. 2016) and relevant for other future low-resolution instrumentation (e.g. ARIEL; Tinetti et al. 2018). Important molecules such as H_2O, CH_4, CO, CO_2, NH_3, N_2, HCN, H_2, O, O_3, O_2, H_2CO, C_2H_2, N_2O_5, N_2O, NO_2 are considered with linelists from HITRAN (Rothman et al. 2013) and HITEMP (Rothman et al. 2010) databases.

3 RESULTS

We model emission and transmission spectra for the three thermal profiles described in Section 2.1 and using Titan's elemental abundances (Section 2.2). The results are shown in Fig. 3. While the difference in the isothermal part of profiles T1 and T2 is only ∼65 K, the difference between T2 and T3 is ∼460 K, which causes large differences in the abundances (Fig. 2) and are also seen in the spectra (Fig. 3). For this reason, profiles T1 and T2 have similar features in emission and transmission, while T3 looks different.

In order to understand the influence of individual species in the spectra, we calculate synthetic spectra with all the species and with all the species except one of them. This is shown in Fig. 4 for emission and in Fig. 5 for transmission.

We show in Fig. 4 that emission spectra present a prominent feature of CO at 4.5–5.5 μm for all three profiles. H_2O features are not relevant in the two hottest cases (T1 and T2) but it has strong features at 5–9 and 13–20 μm in the coldest case (T3). Regarding N-bearing species, NH_3 has features at 10–11 μm only in the coldest case (T3), while HCN features at 3–3.5 and 11–18 μm are more pronounced in the two hottest cases (T1 and T2).

As seen in Fig. 5, we also see strong CO features at 4.5–5.5 μm in transmission spectra. We see NH_3 features at 5.5–6.1 and 8–11 μm, although the former feature is hidden by the stronger H_2O feature at the same wavelength. HCN features are strong at 3.2, 6.1–8 and 11–18 μm. H_2O has strong features at 5–9 and 14–20 μm, although the features at 7–8 and 14–18 μm are hidden by HCN. For the T3 profile, H_2O features at 3–3.8, 4.5–8,5 and 13–20 μm dominate the transmission spectra, with the exception of NH_3 and CO features at 8–13 and 4.5–5.2 μm, correspondingly.

We are probing deep in the atmosphere of 55 Cnc e, at a pressure of ∼1.4 bar (Angelo & Hu 2017). Fig. 6 shows the concentration of the most abundant observable molecules in the atmosphere as a function of the temperature, for a pressure of $P = 1.4$ bar. The figure shows that HCN is the most abundant molecule for T>2100 K, which explains the strong HCN features observed in both emission and transmission for T1 and T2. CO is the second most abundant species for T1 and T2, and also presents strong features. On the other hand, H_2O is not so abundant for T1 and T2, but it becomes more abundant for T3, where we observe the strongest H_2O features. Nevertheless, in all cases in transmission (T1, T2 and T3) and in the coldest case (T3) in emission we observe H_2O features. This is because H_2O is a very strong intrinsic absorber and one of the most important sources for the opacity in the infrared, even if it is not the most abundant molecule in the atmosphere.

N_2 is the most abundant gas in the atmosphere, but it shows no spectral features in transmission or emission, being HCN and NH_3 the N-carriers that show the presence of an N-dominated atmosphere for the three different temperature profiles explored.

3.1 The effect of different atmospheric composition

The origin and atmospheric composition of rocky super-Earths is highly unknown. In the Solar system, the atmospheric composition of rocky bodies is a consequence of accretion of material at early ages and the subsequent outgassing and escape of volatiles during the planet's evolution. One of the parameters that can provide information to trace the history of these bodies is the N/O ratio. In protoplanetary discs, N/O ratio depends on the depletion of N_2 and O-carriers (H_2O, CO_2, CO) and it increases when each of these O-bearing species freezes and the ice-lines are crossed (Piso, Pegues, Öberg 2016). A good example of the relevance of these processes to understand the formation history of the planet is Titan, where it is believed that the present levels of N_2 are a result of accretion of primordial NH_3 ices present in the protosolar nebula (Atreya, Donahue & Kuhn 1978; Mandt et al. 2014). For this reason,

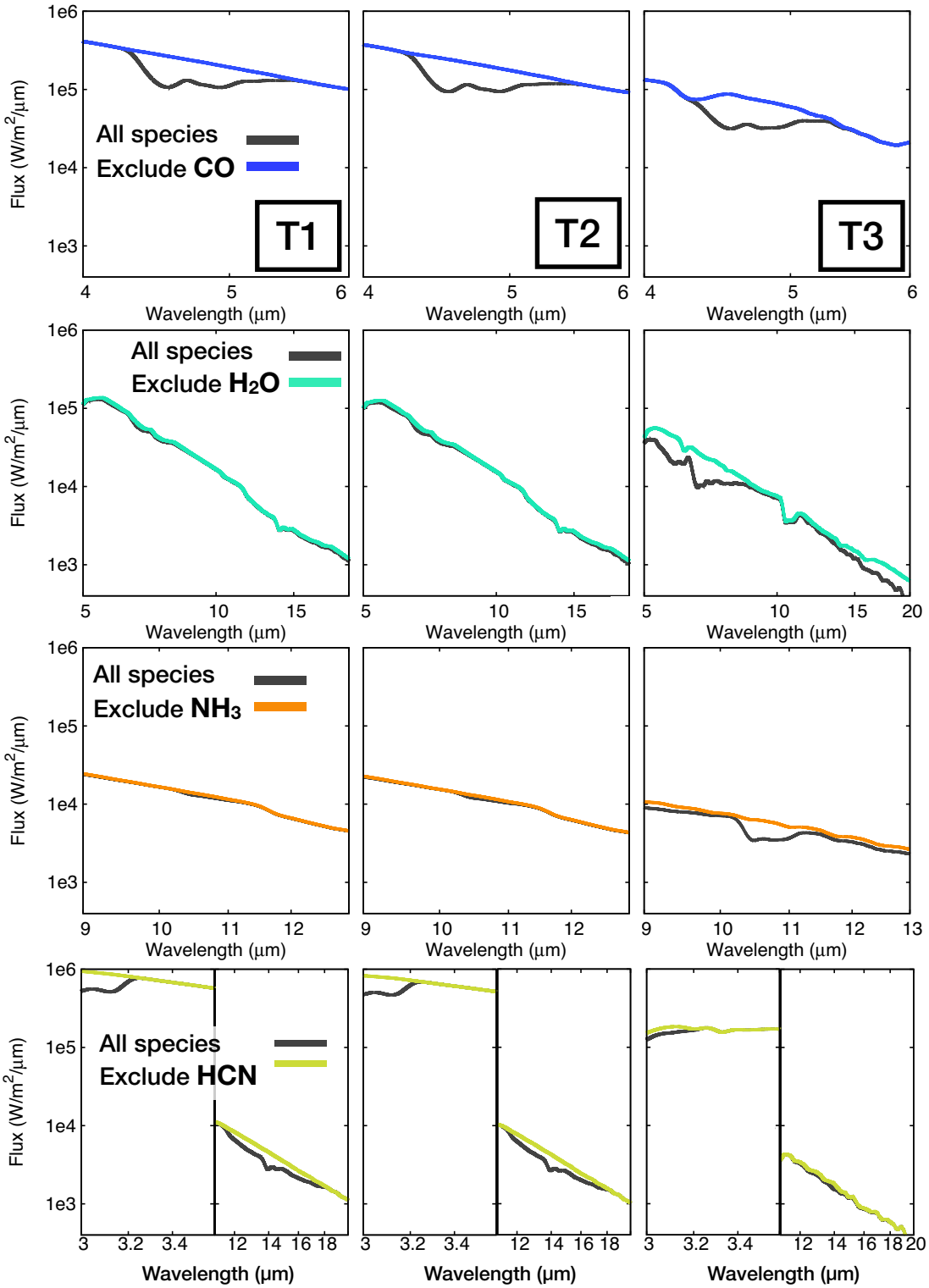

Figure 4. Spectral features in emission for the most relevant species and for the three different cases: profile T1 (left), T2 (middle) and T3 (right column). Spectra including all species is shown in grey and spectra with all species but excluding one of them is shown in colours (same colour code as in Fig. 2). Note that in order to highlight the individual features of different species, we show a different wavelength range in the different rows. HCN is divided in two to show its two relevant features.

and due to the high uncertainties in the composition of 55 Cancri e's atmosphere, we explore different N/O ratios maintaining an N-dominated atmosphere, to explore the changes in the chemistry and assess possible observability with future instrumentation.

In addition to Titan's N/O $= 3.85 \times 10^4$ (see Section 2.2), we also explore two other cases: N/O $= 3.85 \times 10^3$ and N/O $= 3.85 \times 10^2$, maintaining Titan's abundances for C and H. In these two additional cases we use profile T2. Fig. 7 shows the change

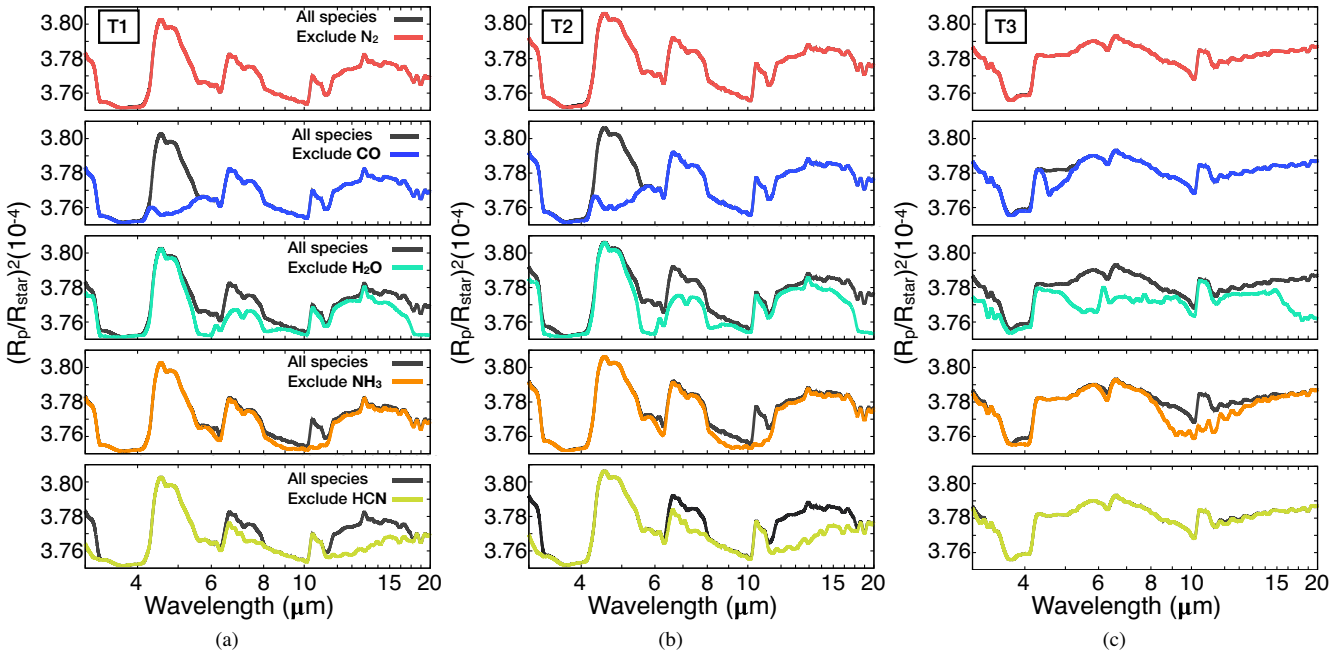

Figure 5. Transmission synthetic spectra for profile T1 (left), T2 (middle) and T3 (right panel). Same colour code as in Fig. 4.

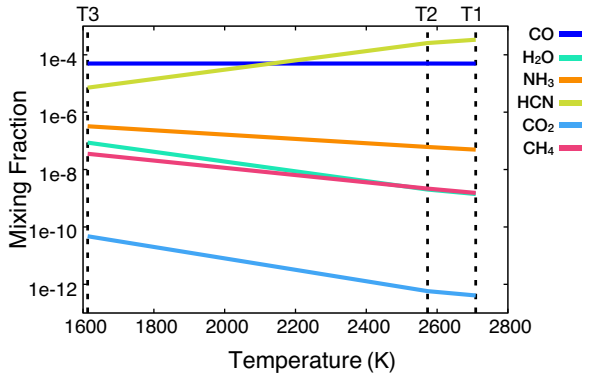

Figure 6. Mixing fraction of the most abundant observable molecules in the atmosphere (CO, H_2O, NH_3, HCN, CO_2,CH_4) as a function of temperature at a pressure of 1.4 bar.

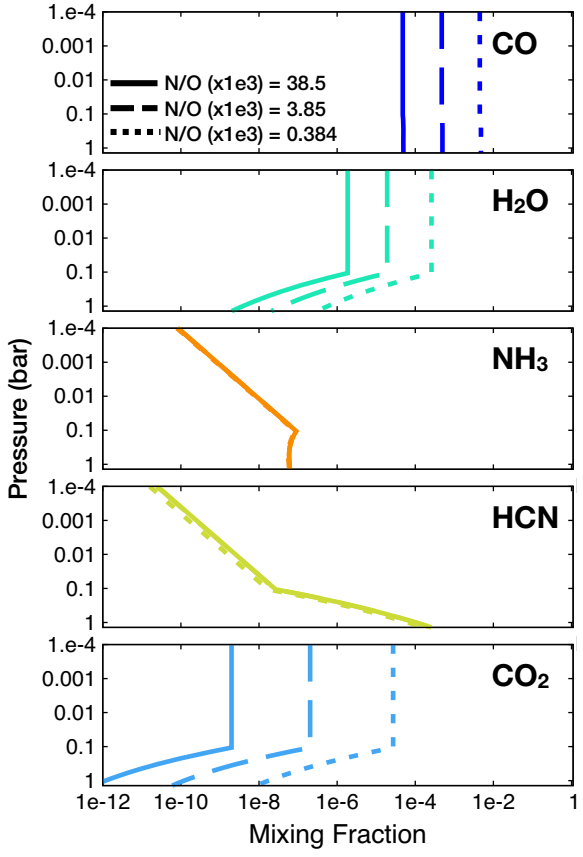

Figure 7. Mixing fractions of some relevant O- and N-carriers in the atmosphere. Different panels show different species and different lines represent the three different N/O ratios explored.

in the atmospheric chemistry. We see that an increase in O leads to a larger concentration of CO, H_2O, and specially CO_2, which increases ∼2 orders of magnitude. On the other hand, even though the percentage of N is lower, we do not see any significative change in NH_3 and HCN concentrations.

These differences in concentrations are seen in the spectra (Fig. 8). The relevance of each individual species in the spectra is shown in Fig. 9 for emission and in Fig. 10 for transmission spectra.

Fig. 9 shows that CO features grow in strength when decreasing N/O in the emission spectra. The same happens with H_2O and CO_2, which was not even relevant for the largest N/O case that we considered in Section 3. NH_3 has no features in the three cases, while HCN features weaken when decreasing N/O.

For transmission, we see in Fig. 10 that a decrease in N/O leads to stronger H_2O and CO features. CO_2 features were not observable in the transmission spectra of Titan's N/O, but they become noticeable as we decrease the N/O. On the other hand, we see weaker NH_3

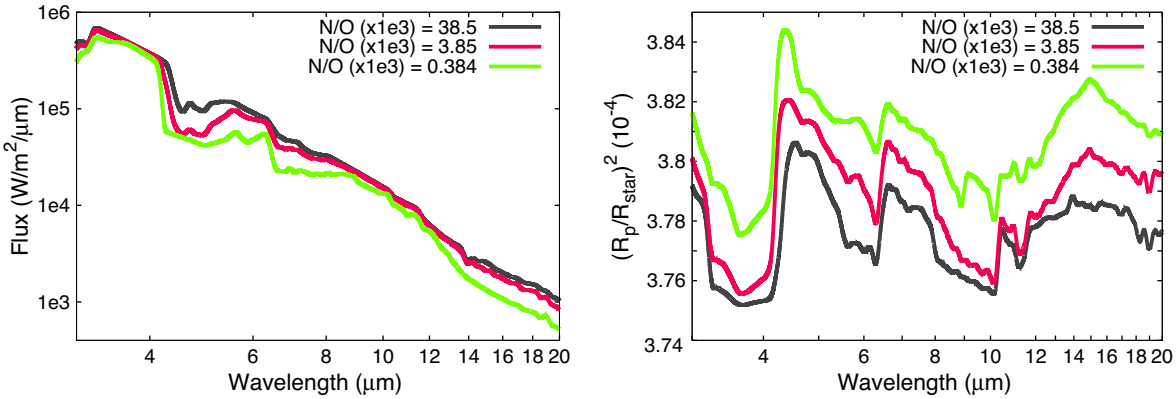

Figure 8. Emission (left) and transmission (right panel) spectra calculated using three different N/O ratios in the atmosphere.

and HCN features when decreasing the N/O. Interestingly, NH_3 and HCN vanish in the case with the smallest N/O, implying that if O levels are high enough, we cannot observe any N-carrier in the transmission spectra in an N-dominated atmosphere. We also see that the R_p/R_{star} increases as N/O decreases, therefore a large N/O is more consistent with phase curve observations (Angelo & Hu 2017).

4 DISCUSSION

4.1 Disequilibrium chemistry

The abundances of different species in 55 Cancri e atmosphere were calculated assuming that the atmosphere is in chemical equilibrium, which is usually a good approximation for extremely hot planets (Line & Yung 2013; Miguel & Kaltenegger 2014; Venot et al. 2018). Detailed calculations including disequilibrium processes are beyond the scope of this paper and will be included in a future study. We introduce this analysis to discuss its main effects and how this might affect our calculations

Due to the close proximity between the planet and the host star, dissociation of atmospheric species is probably one of the most important disequilibrium processes that occur in this atmosphere. This process requires an energy above the dissociation energy for each molecule, and the effectiveness of this process will also depend on the absorption cross-section of each molecule at those energies. Fig. 11 shows the absorption cross-sections of some of the most relevant species in the atmosphere. N_2 is a very stable molecule; its dissociation threshold is around 0.1265 μm (Yung & Demore 1999) and, as seen in Fig. 11, N_2 has a large cross-section for wavelengths $\lambda < 0.1$ μm. This energy is probably absorbed higher in the atmosphere, so is likely that this process plays no important role in the chemistry at $P<1 \times 10^{-4}$. The other N-carrier of relevance is NH_3; this molecule has a dissociation threshold at 0.2637 μm (Yung & Demore 1999) and its absorption is important for $\lambda \sim 0.2$ μm, where it has no other competitor, so this molecule will probably dissociate and form NH_2 +H. In Fig. 5 we show how the spectra would look like without NH_3 being present in the atmosphere, although we note that its dissociation might affect other molecules as well. Finally, we have CO and H_2O. CO has a very strong bond with a dissociation energy at 0.1113 μm (Yung & Demore 1999), similar to the case of N_2; this energy is likely to be absorbed higher in the atmosphere. H_2O is not so abundant (see Fig. 2), but since its dissociation threshold is at 0.2398 μm (Yung & Demore 1999), it is likely to dissociate in this atmosphere for $\lambda \sim 0.17$ μm. Fig. 5 shows the spectra with no H_2O.

Including the effects of photochemistry might be important for understanding the chemistry and its effects on the spectra of hot rocky exoplanet atmospheres, especially for planets around active stars that emit strongly in the UV.

5 CONCLUSION

Observations of 55 Cancri e suggest the presence of a high-mean-molecular-weight atmosphere (Ehrenreich et al. 2012; Demory et al. 2016). A subsequent analysis of those observations and 3D modelling further supports the idea of an N-dominated atmosphere (Angelo & Hu 2017; Hammond & Pierrehumbert 2017). In this context, this paper makes a first approximation to explore an N-dominated atmosphere for 55 Cancri e and study its most relevant molecules and spectral features for transmission and emission spectroscopy in views of future observations (JWST, ARIEL).

Since hot super-Earths atmospheres are largely unknown, we use three different extreme atmospheric thermal profiles, calculated using an analytical approach and parameters derived from observations (Angelo & Hu 2017; Crida et al. 2018). We adopt as an example of an N-atmosphere Titan's elemental abundances and calculate the chemistry using equilibrium chemistry. We also test the effect of changing the elemental abundances composition decreasing the N/O ratio. Finally, we compute transmission and emission spectra to a low-resolution comparable to what we will be able to obtain with future instrumentation.

Our results show that N_2 is the most abundant molecule in the atmosphere for all pressures, followed by H_2, CO and H_2O, where CO is more relevant for the hottest profiles and H_2O for the coldest case (for $P<0.1$ bar). The effect of decreasing N/O ratio is an increase in H_2O, CO and CO_2 and a decrease in NH_3 and HCN abundances.

Both emission and transmission spectra show strong CO features at 4.5–5.5 μm for the three thermal profiles. H_2O features are also visible at 5.5–6.1 and 18–20 μm for all cases considered in transmission and for the coldest case (T3) in emission. Regarding N-bearing species, N_2 shows no features, but other N-bearing species, not so abundant but strong absorbers, can be seen in the spectra. These are NH_3 and HCN, both with strong features. NH_3 features are at 8–11 μm for the three profiles in transmission and for the coldest profile (T3) in emission. HCN features are at 3, 6.1–8 and 11–18 μm, although are only strong for the two hot cases both in transmission

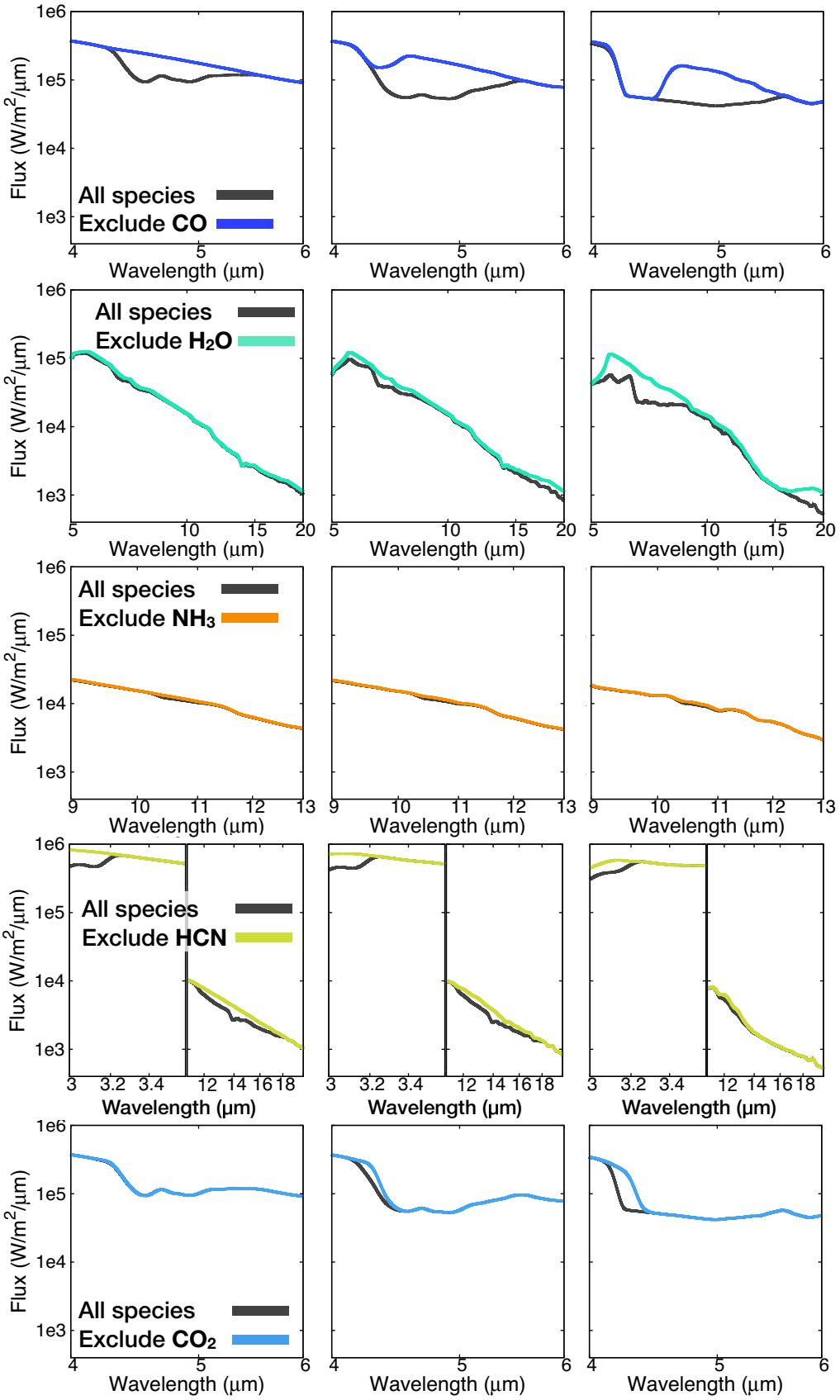

Figure 9. Effect of different species in the emission spectra and how they change with different N/O ratios. We show results with N/O $= 3.85 \times 10^4$ (left), N/O $= 3.85 \times 10^3$ (centre) and N/O $= 3.85 \times 10^2$ (right column). Same colour code as in Fig. 4.

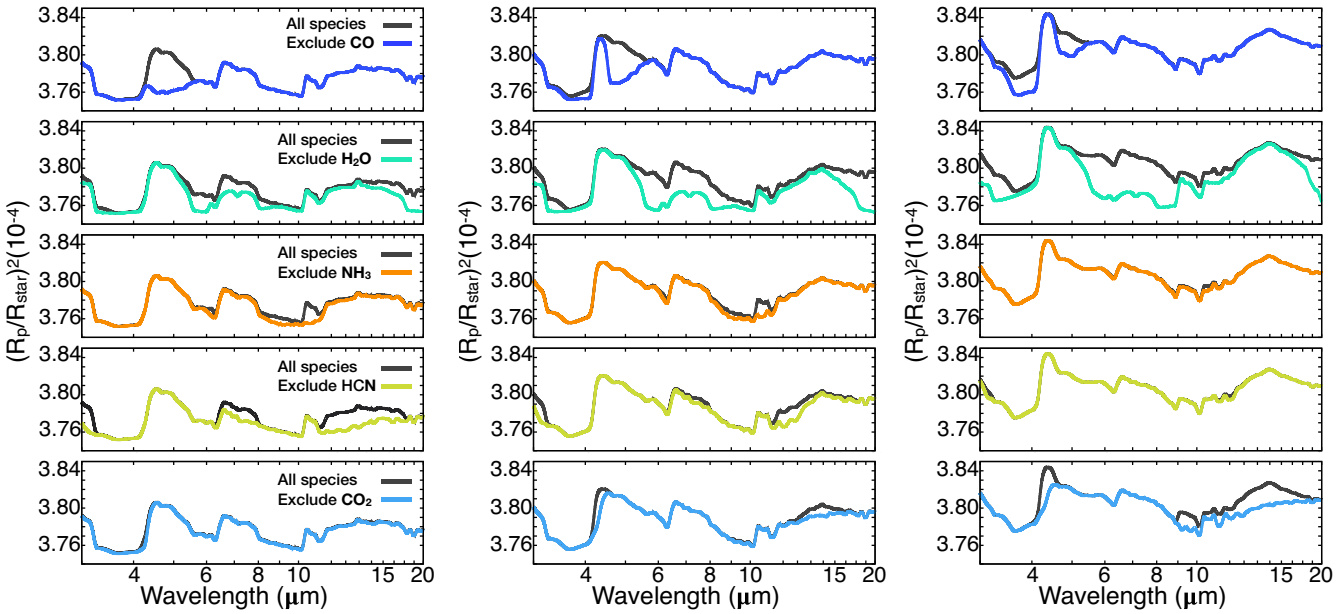

Figure 10. Consequence of a change in the N/O ratio in the transmission spectra. We show spectra adopting N/O $= 3.85 \times 10^4$ (left), N/O $= 3.85 \times 10^3$ (centre) and N/O $= 3.85 \times 10^2$ (right panel) in the atmosphere. The spectra including all the species are shown in grey and the spectra excluding a specific molecule (indicated in the figure on the left panel, same for the other panels) is shown in colours.

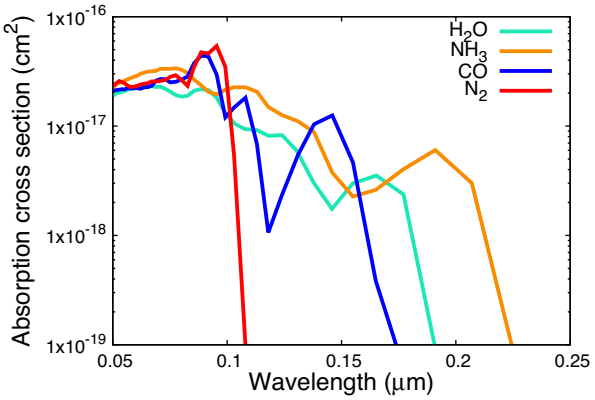

Figure 11. Absorption cross-sections of some of the most relevant molecules in the atmosphere: N_2 (Chan et al. 1993a), NH_3 (Burton et al. 1993), CO (Chan, Cooper & Brion 1993c) and H_2O (Chan, Cooper & Brion 1993b).

and emission. When decreasing the N/O, we observe stronger features of H_2O, CO and CO_2 and weaker features of NH_3 and HCN. The case with the smallest N/O ratio shows no N-carrier molecules in transmission spectra and weak HCN lines in emission. We also find that a large N/O ratio is more consistent with observations.

Our results can be used as a guide to understand what to expect in an N-dominated atmosphere for 55 Cancri e and as a reference in preparation for future observations.

ACKNOWLEDGEMENTS

The author wants to thank Ignas Snellen and the exoplanets group at Leiden Observatory for valuable comments that helped to improve this paper.

REFERENCES

Angelo I., Hu R., 2017, AJ, 154, 232
Atreya S. K., Donahue T. M., Kuhn W. R., 1978, Science, 201, 611
Blecic J., Harrington J., Bowman M. O., 2016, ApJS, 225, 4
Bourrier V. et al., 2018, A&A, 619, A1
Burton G. R., Chan W. F., Cooper G., Brion C. E., 1993, Chem. Phys., 177, 217
Chan W. F., Cooper G., Sodhi R. N. S., Brion C. E., 1993a, Chem. Phys., 170, 81
Chan, W. F., Cooper, G., Brion, C. E., 1993b, Chem. Phys., 178, 387
Chan W. F., Cooper G., Brion C. E., 1993c, Chem. Phys., 170, 123
Crida A., Ligi R., Dorn, C., Lebreton Y., 2018, ApJ, 860, 122
Cridland A. J., Pudritz R. E., Alessi M., 2016, MNRAS, 461, 3274
Demory B.-O. et al., 2011, A&A, 533, A114
Demory B.-O. et al., 2016, Nature, 532, 207
Ehrenreich D. et al., 2012, A&A, 547, A18
Espinoza N., Fortney J. J., Miguel Y., Thorngren D., Murray-Clay R., 2017, ApJ, 838, L9
Esteves L. J., de Mooij E. J. W., Jayawardhana R., Watson C., de Kok R., 2017, AJ, 153, 268
Greene T. P. et al., 2016, ApJ, 817, 17
Hammond M., Pierrehumbert R. T., 2017, ApJ, 849, 152
Kaltenegger L., Traub W. A., Jucks K. W., 2007, ApJ, 658, 598
Kaltenegger L., Traub W. A., 2009, ApJ, 698, 519
Line M. R., Yung Y. L., 2013, ApJ, 779, 3
Madhusudhan N., Bitsch B., Johansen A., Eriksson L., 2017, MNRAS, 469, 4102
Mahapatra G., Helling C., Miguel Y., 2017, MNRAS, 472, 447
Mandt K. E., Mousis O., Lunine J., Gautier D., 2014, ApJ, 788, L24
Miguel Y., Kaltenegger L., 2014, ApJ, 780, 166
Miguel Y., Kaltenegger L., Fegley B., Schaefer L., 2011, ApJ, 742, L19
Morley C. V., Kreidberg L., Rustamkulov Z., Robinson T., Fortney J. J., 2017, ApJ, 850, 121
Nelson B. E. et al., 2014, MNRAS, 441, 442
Öberg K. I., Murray-Clay R., Bergin E. A., 2011, ApJ, 743, L16
Pierrehumbert R. T., 2010, Principles of Planetary Climate, Cambridge University Press, ISBN:9780521865562

Piso A., Pegues J., Öberg, K., 2016, ApJ, 833, 203
Ridden-Harper A. R. et al., 2016, A&A, 593, A129
Rothman L. et al., 2010, J. Quant. Spectrosc. Radiat. Transf., 111, 2139
Rothman L. S. et al., 2013, J. Quant. Spectrosc. Radiat. Transf., 130, 4
Rugheimer S., Kaltenegger L., 2018, ApJ, 854, 19
Rugheimer S. et al., 2013, Astrobiology, 13, 251
Schaefer L., Fegley B., 2009, ApJ, 703, L113
Tinetti G. et al., 2018, Exper. Astron., 1
Traub W. A., Stier M. T., 1976, Applied Optics, 15, 364
Traub W. A., Jucks K., 2002, in Mendillo M., Nagy, A., Waite J. H., eds, Atmospheres in Geophys. Monogr. 130, The Solar System: Comparative Aeronomy. AGU, Washington, DC, p. 369
Tsiaras A. et al., 2016, ApJ, 820, 99
Venot O. et al., 2018, Exper. Astron.accepted
Wang D., Miguel Y., Lunine J., 2017, ApJ, 850, 199
Winn J. N. et al., 2011, ApJ, 737, L18
Yung Y. L., Demore W. B., 1999, Photochemistry of Planetary Atmospheres. Oxford University Press, New York,p. QB603.A85 Y86

This paper has been typeset from a TEX/LATEX file prepared by the author.